

# The Effect of Humidity Levels on Carbon Dioxide Gas Concentration Measurement using a Titanium Dioxide-Coated Quartz Crystal Microbalance

Laili Mardiana<sup>1</sup>, Arinto Yudi Ponco Wardoyo<sup>2\*</sup>, Masruroh<sup>2</sup>, Hari Arief Dharmawan<sup>2</sup>

<sup>1</sup>Faculty of Natural Science and Mathematics, University of Mataram, Indonesia

<sup>2</sup>Faculty of Natural Science and Mathematics, University of Brawijaya, Indonesia

\*Author to whom correspondence should be addressed:

E-mail: a.wardoyo@ub.ac.id

(Received March 01, 2023; Revised January 22, 2024; Accepted February 19, 2024).

**Abstract:** Carbon dioxide (CO<sub>2</sub>) is an odorless and colorless gas in ambient air. Carbon dioxide is one of the greenhouse gases that is related to climate change. Carbon dioxide gas is released by many sources and exhaled by humans and animals in ambient air. Carbon dioxide gas concentration can be measured using several techniques. However, the most important thing is the ability to measure carbon dioxide gas concentration in a high-humidity environment, such as high-cost maintenance, specific operators, sensor replacement, decreased performance, and many others. In line with this, this study aimed to develop a carbon dioxide gas sensor using a quartz crystal microbalance and TiO<sub>2</sub> layer. This study also identified the influence of the humid environment on the sensor's performance. The TiO<sub>2</sub>-coated quartz crystal microbalance sensor was installed inside a box and connected to a frequency counter to measure the frequency shifts. Then, the sensor was exposed to the sample gas (concentration = 10,000 mL/m<sup>3</sup>) with varied humidity levels: 60%, 69%, 79%, 89%, and 99%. The humidity variations were controlled using a humidity level controller. These sensor evaluations were conducted inside an experimental chamber. The results show that the low humidity levels (60% and 69%) have the fastest response times (1 s). The high humidity levels (89% and 99%) show the slowest response time (6 s). The best accuracy (75%) and sensitivity levels (0.0045 Hz/ppm) are obtained from the low humidity level (60%). It can be concluded that the TiO<sub>2</sub>-coated quartz crystal microbalance sensor can be used as a carbon dioxide gas sensor with a humidity <80%. The humidity level influences the sensitive layer of the sensor due to the existence of water molecules. A lower humidity level, a higher sensor performance.

Keywords: carbon dioxide; humidity; quartz crystal microbalance; titanium dioxide

## 1. Introduction

The impact of global warming is commonly identified by the average Earth's surface temperature increase. Global warming is also related to greenhouse gases<sup>1-3</sup>. The biggest contributor of greenhouse gases is carbon dioxide or CO<sub>2</sub> gas (72%)<sup>4,5</sup>. The increase in CO<sub>2</sub> gas is found in many regions, including Indonesia, Japan, Thailand, and other countries. The increase of CO<sub>2</sub> gas is influenced by the increase of emission sources, such as transportation, population, and industrial sectors<sup>6-10</sup>.

A previous study identified that CO<sub>2</sub> gas in the atmosphere reached 410.40 ppm<sup>11</sup>. The increase in CO<sub>2</sub> gas is related to a serious health impact when the concentration is > 500 ppm<sup>12</sup>. Another previous study shows a significant increase in CO<sub>2</sub> gas concentration (about 2 ppm per year). The increase of this gas is related to several diseases, such as oxidative stress and endothelial dysfunction. Hence, a way to overcome this

problem is by conducting a monitoring or mitigation system.

CO<sub>2</sub> gas concentrations are measured using many technologies, such as a metal oxide gas sensor<sup>13</sup>, micro-electro-mechanical systems (MEMS)<sup>14</sup>, non-dispersive infrared (NDIR)<sup>15</sup>, QCM (quartz crystal microbalance)<sup>16</sup>, and many others. NDIR is a low-cost principle with a compact size, easy process control, continuous measurement, and high sensitivity. However, the most disadvantage of this principle is unstable measurement due to the influence of humidity and temperature changes<sup>17</sup>. In contrast, a QCM-based sensor has an advantage in its high sensitivity, real-time, and rapid response. A QCM also has rapid recovery times, good linearity, high stability, and good control for humidity parameters<sup>18</sup>.

## QCM Working Principle

A QCM sensor has a specific fundamental frequency ( $f_0$ ) that depends on the electrode's material and crystal characteristics. QCM works due to the mass deposition on its surface with the principle of quartz crystal frequency<sup>18)</sup>. In other words, a QCM crystal is a mass sensor where the measured frequency decreases linearly to the mass changes<sup>19)</sup>. QCM-based sensors are also easy to develop due to the flexibility of surface modification using many functional layers<sup>20)</sup>. The surface modification is related to the QCM performance as the sensing element since a bare QCM performs as a mass detection only. For a specific analyte or targeted substance, the surface of the QCM has to be modified or coated using a sensitive material that can react with the targeted substances<sup>21,22)</sup>. Due to this characteristic, QCM has the potential to be developed as a gas sensor using a specific coating material.

## Titanium Dioxide (TiO<sub>2</sub>) as a Sensitive Layer

One of the most popular QCM coating materials or layers is titanium dioxide (TiO<sub>2</sub>). TiO<sub>2</sub> has good chemical stability and low toxicity. TiO<sub>2</sub> is relatively considered a low-cost material with a unique characteristic<sup>23)</sup>. TiO<sub>2</sub> is easy to be modified for a sensor development with a good electronic and optic characteristics<sup>24,25)</sup>. The TiO<sub>2</sub> layer has been used as a CO<sub>2</sub> sensor with varied performances. However, recent studies have yet to identify the humidity or moisture content effect on the sensor's performance, since humidity level is important in atmospheric gas measurement<sup>17)</sup>. Moreover, a good sensor that performs well in a humid environment is also important. In line with this, this study aims to develop a CO<sub>2</sub> gas sensor using a titanium dioxide layer. This study also identifies the influence of humidity on the sensor's performances, including accuracy, sensitivity, linearity, and response time.

## 2. Materials and Methods

### 2.1. Sensor Preparation

This study used QCMs (base frequency  $f_0 = 4.995$  MHz, silver electrodes, purchased from PT. Great Microtama Electronics Indonesia) as the bare sensors. All QCMs

were coated using nano-TiO<sub>2</sub> layers (anatase phase, 2 molars) diluted in aquabides. The coating process was conducted using a spin coating method (5 μL, 500 rotation per minute for 10 s and 2500 rotation per minute for 60 s). The coated QCMs were naturally air-dried inside a vacuum chamber and tested using a frequency counter<sup>26,27)</sup>. The surface of the coated QCMs were characterized using a SEM (scanning electron microscope, JEOL-JCM7000). The as-prepared sensor was installed in a sensor box (Fig. 1).

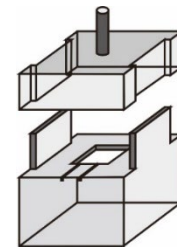


Fig. 1: The schematic design of the QCM box.

### 2.2. CO<sub>2</sub> Gas Measurement

The performances of the QCM sensors were evaluated using pure CO<sub>2</sub> gas (Fig. 2, purity = 99.98%, purchased from PT. Malson Gas Indonesia) inside an experimental chamber (volume  $V = 0.03$  m<sup>3</sup>, flow rate  $Q = 1$  L/minute). The gas humidities were varied into five variations (60%, 69%, 79%, 89%, and 99%) using a humidifier (humidity controller) to investigate the influence of humidity level on CO<sub>2</sub> measurement. For the first step, the humidifier was connected to the gas tube and set to 60%. The gas sample was injected into the experimental chamber with a constant  $Q$  (1 L/minute) for 18 s. This step generated 300 ml of CO<sub>2</sub> gas inside the chamber (concentration = 10,000 mL/m<sup>3</sup>). The sensor was installed inside the experimental chamber and connected to a frequency counter to measure the frequency shift ( $\Delta f$ ). These processes were also conducted to identify the response ( $t_{rs}$ ) and recovery times ( $t_{rc}$ ). These treatments were conducted for all humidity variations. The humidity and temperature levels were measured using a digital sensor.

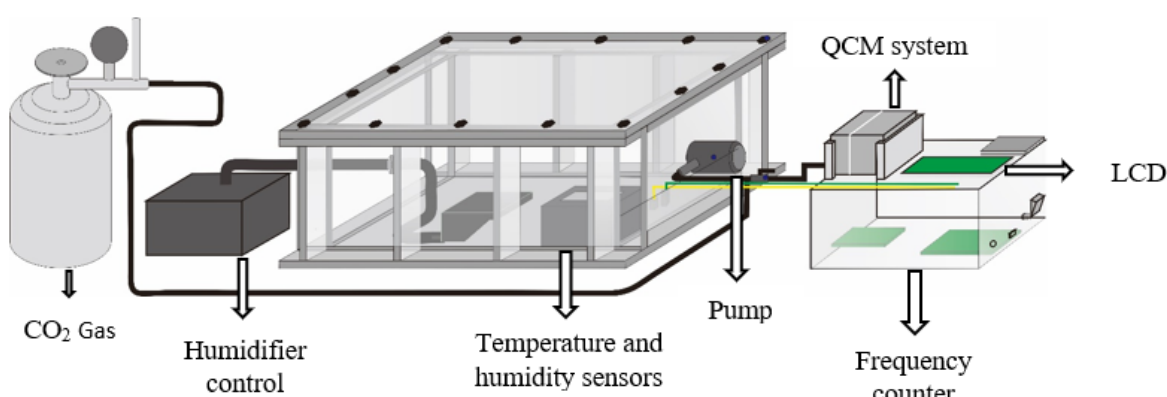


Fig. 2: Experiment setup for the performance test.

### 2.3. Performance Evaluation

All data were written as the mean and SD (standard deviation). The frequency shift of each sensor ( $\Delta f$ ) was calculated from the difference between  $f_0$  and  $f^{(8)}$ . According to Sauerbrey's equation, a higher frequency shift interprets more deposited  $\text{CO}_2$  gas. The deposited mass,  $\Delta m$ , is linear to the frequency shift ( $\Delta f$ ) (Eq. 1).  $A$  is the area of the sensor's electrodes, while  $\mu_q$  ( $2.947 \times 10^{11} \text{ g/cm s}^2$ ) and  $\rho_q$  ( $2.648 \text{ g/cm}^3$ ) are the shear modulus and density of the quartz, respectively. The accuracy level was calculated by comparing the gas concentration ( $10,000 \text{ mL/m}^3$ ) and deposited gas mass ( $\Delta m$ ). The differences in the sensor's frequency responses in measuring the gas concentrations were evaluated using a one-way ANOVA (analysis of variance) test, where  $p < 0.05$  was considered statistically different.

$$\Delta m = -\frac{A \sqrt{\rho \mu}}{2 f_0^2} \cdot \Delta f \quad (1)$$

## 3. Results

### 3.1. Surface observation

Figure 3 shows the sensor's morphology with the  $\text{TiO}_2$  layer. It can be seen that there is a rigid and uniform layer on the surface. The particle distribution is observed at  $\pm 200 \text{ nm}$  (classified as fine particle).

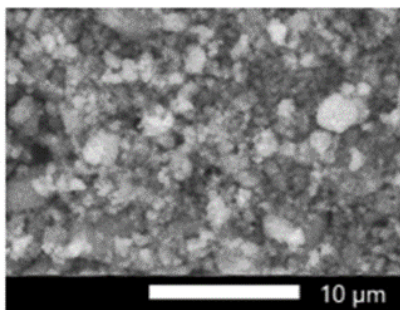


**Fig. 3:** Morphological images of  $\text{TiO}_2$  on the QCM surface (Scale bar =  $10 \mu\text{m}$ ).

According to the measurement, the initial frequency of a bare QCM sensor is  $4.995 \text{ MHz}$ . The measured frequency of the QCM after being coated is  $4.990 \text{ MHz}$ . The frequency difference is about  $5.135 \text{ kHz}$ . This low-frequency difference indicates a low impedance due to a stable oscillation frequency, a uniform surface, and a rigid surface. In other words, the titanium dioxide was successfully coated on the QCM's surface ( $0.259 \mu\text{m}$ ).

$\text{TiO}_2$  coating is a technique to increase the performance of a QCM sensor. As a requirement in developing a selective gas sensor, a QCM's surface must be analyzed, including the roughness level, particle distribution, and coating thickness<sup>29</sup>. A nanometer-scale particle is useful for getting a bigger volume fraction and higher porosity. As an impact, it may increase the adsorption ability<sup>30</sup>.

### 3.2. Frequency and response times

Figure 4 shows the sensor's responses under different humidity levels. This figure interprets that the first humidity variation (60%) has the fastest response time. This variation has only  $1 \text{ s}$  in giving the first response under  $\text{CO}_2$  gas concentration ( $\Delta f = -45 \text{ Hz}$ ). The second position belongs to the second humidity variation (69%), showing a response time of  $1 \text{ s}$  ( $\Delta f = -34 \text{ Hz}$ ). The third humidity variation (79%) shows the third position:  $2 \text{ s}$  ( $\Delta f = -32 \text{ Hz}$ ). Both 89% and 99% humidity levels do not interpret good response times (the response times are  $6 \text{ s}$ ). These two humidity variations have low-frequency shifts ( $\Delta f < 30 \text{ Hz}$ ). The fastest response time shows the best sensor response under  $\text{CO}_2$  gas. Then, the biggest frequency shift also indicates better gas detection using a QCM sensor ( $p < 0.05$ ).

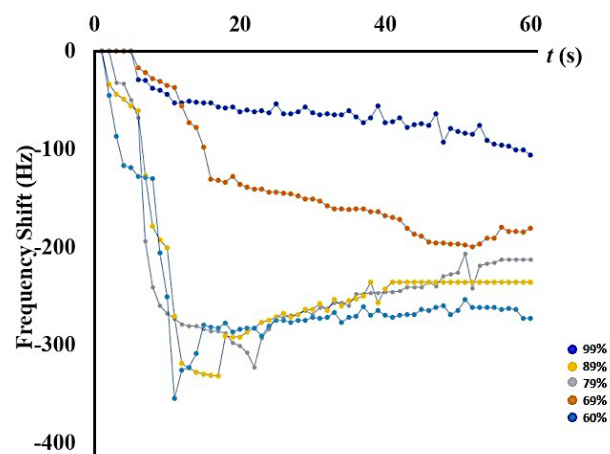


**Fig. 4:** Frequency responses of the QCM sensors under humidity levels

### 3.3. Sensitivity and accuracy levels

Figure 5 interprets the accuracy and sensitivity levels of the sensors under different humidity levels. It can be seen that the first, second, and third humidity variations have accuracy levels  $> 70\%$ . These humidity levels also have good sensitivities,  $0.0032\text{-}0.0045 \text{ Hz/ppm}$ . In contrast, 89% and 99% humidity levels have low accuracy ( $< 70\%$ ) and sensitivity levels ( $< 0.0030 \text{ Hz/ppm}$ ). A higher sensitivity level indicates a better sensor response. Meanwhile, a higher accuracy level indicates a better sensing result in a measurement system.

## 4. Discussion

The results indicate that the QCM and  $\text{TiO}_2$  layer can be fabricated as a  $\text{CO}_2$  gas sensor. According to the sensitivity and accuracy levels, including the response time, it can be seen that the system performances are related to the humidity variations. Thus, the sensitive layer and the humidity levels influence the sensing parameters.

The  $\text{TiO}_2$  layer has specific crystal phases that influence the material sensitivity regarding  $\text{CO}_2$  or other analytes.

This characteristic can be applied as a sensitive layer for sensor development using a QCM. Generally, a QCM sensor has three working phases: active zone (frequency decreases linearly to the increasing deposited mass), steady state (maximum resonance), and recovery state (back to initial frequency). In this study, the sensor might have a maximum condition or steady state and relaxation time when exposed to  $\text{CO}_2$  gas.

The sensing mechanism of  $\text{CO}_2$  gas with a  $\text{TiO}_2$  layer is related to oxygen adsorption (Fig. 6). This mechanism can be investigated in the surfaces of the QCM when exposed to  $\text{CO}_2$  gas (both physisorption and chemisorption processes)<sup>22</sup>. These two reactions are related to the temperature fluctuation (as well as the humidity level) and oxygen molecules. Oxygen molecules may adsorb on the surface of the  $\text{TiO}_2$ -coated QCM sensor by the physisorption process due to Van der Waals bond. There will be several dipole interactions that can adsorb oxygen molecules. As a chain reaction, there will be new substances: chemisorbed oxygen species ( $\text{O}_2^-$ ) on the QCM electrodes. Since QCM is a microbalance crystal, adding mass to its surface causes a decreasing frequency. When the maximum resonance occurs (due to the bindings of the oxygen atom from humidity and the Ti atom), it causes a stagnant response in the QCM sensor (humidity > 79%) and the sensor cannot reach the initial frequency<sup>31,32</sup>. In other words, the sensor optimally works at the humidity <80%.

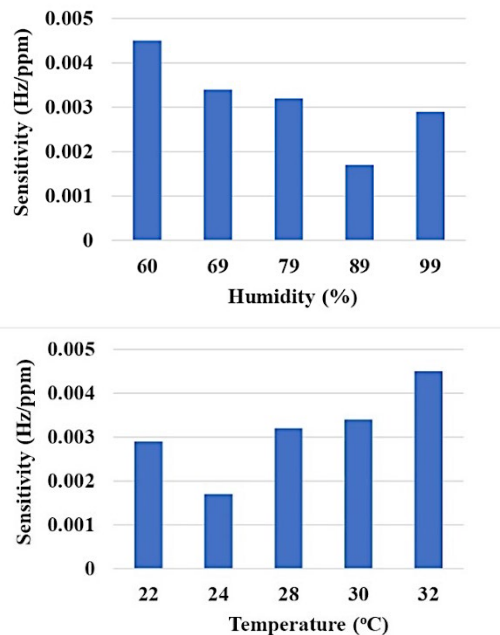


Fig. 5: Sensitivity levels: (a). humidity; and (b). temperature.

The most problem of the measurement is the issue of water molecules. Hence, more  $\text{CO}_2$  exposure with high moisture content might cause a maximum resonance on the sensor's electrodes. When  $\text{TiO}_2$  reacts with humid  $\text{CO}_2$ , the moisture content is observed on the sensor's surface and interacts with  $\text{TiO}_2$ . This interaction may generate a new layer (with water molecules) due to the hydroxyl

group<sup>33</sup>. As the impacts, this interaction may decrease the flexibility and reversibility of the sensor (as found in the high humidity levels). These results indicate that the high humidity levels (80-99%) have low sensitivity and accuracy levels due to the mass-loading effect.

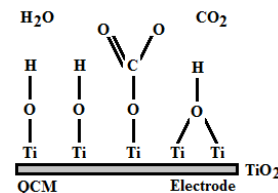


Fig. 6: Interactions between  $\text{TiO}_2$  and  $\text{CO}_2$  and  $\text{H}_2\text{O}$ .

## 5. Conclusion

In summary, a  $\text{CO}_2$  gas sensor using a  $\text{TiO}_2$ -coated QCM is fabricated and evaluated under different humidities: 60%-99%. The humidity variations are used to identify the influence of the humid environment in the sensing performances. The sensor works well in detecting and measuring  $\text{CO}_2$  gas concentration with humidity <80%. The fastest response time, 1 s, is obtained at the humidity level of 60-69% (accuracy >70%). The sensitivity levels are 0.0017 to 0.0045 Hz/ppm. A lower humidity has a higher sensor performance in sensing  $\text{CO}_2$  gas.

## Acknowledgments

All authors thank the University of Mataram (Mataram, West Nusa Tenggara, Indonesia) for the financial support. The kind hands of the members of the Laboratory of Air Quality and Health Impacts (Physics Department, University of Brawijaya, Malang, Indonesia) are acknowledged.

## Nomenclature

$\Delta m$	deposited mass ( $\mu\text{g}$ )
$t_{rs}$	response time (s)
$f_0$	fundamental frequency (Hz)
$f$	frequency (Hz)
$\Delta f$	frequency shift (Hz)
$Q$	flow rate ( $\text{m}^3/\text{s}$ )

## References

- 1) G. Chen, J. Bai, C. Bi, Y. Wang, and B. Cui, "Global greenhouse gas emissions from aquaculture: a bibliometric analysis," *Agric Ecosyst Environ*, 348 (January) 108405 (2023). doi:10.1016/j.agee.2023.108405.
- 2) Y. Zhang, C. Song, X. Wang, N. Chen, G. Ma, H. Zhang, X. Cheng, and D. Sun, "How climate warming and plant diversity affect carbon greenhouse gas

emissions from boreal peatlands: evidence from a mesocosm study," *J Clean Prod*, 404 (March) 136905 (2023). doi:10.1016/j.jclepro.2023.136905.

- 3) Q.H. Phung, K. Sasaki, Y. Sugai, M. Kreangkrai, and T. Babadagli, "Numerical simulation of CO<sub>2</sub> enhanced coal bed methane recovery for a Vietnamese coal seam," *Evergreen*, 2 1–7 (2010).
- 4) A. Saiful, A.T. Wijayanta, K. Nakaso, and J. Fukai, "Predictions of O<sub>2</sub>/N<sub>2</sub> and O<sub>2</sub>/CO<sub>2</sub> mixture effects during coal combustion using probability density function," *Evergreen*, 2 12–16 (2010).
- 5) C. Moro, V. Franciosi, M. Lopez-Arias, and M. Velay-Lizancos, "The impact of CO<sub>2</sub> uptake rate on the environmental performance of cementitious composites: a new dynamic global warming potential analysis," *J Clean Prod*, 375 (September) 134155 (2022). doi:10.1016/j.jclepro.2022.134155.
- 6) H. Guo, J. Jiang, Y. Li, X. Long, and J. Han, "An aging giant at the center of global warming: population dynamics and its effect on CO<sub>2</sub> emissions in China," *J Environ Manage*, 327 (February 2022) 116906 (2023). doi:10.1016/j.jenvman.2022.116906.
- 7) J. Wu, O.J. Abban, A.D. Boadi, E.A. Addae, M. Akhtar, Y. Hongxing, and C. Ofori, "Time–frequency contained co-movement of renewable electricity production, globalization, and CO<sub>2</sub> emissions: a wavelet-based analysis in Asia," *Energy Reports*, 8 15189–15205 (2022). doi:10.1016/j.egyr.2022.11.054.
- 8) I. V. Filimonova, A. V. Komarova, V.M. Kuzenkova, I. V. Provornaya, and V.D. Kozhevnik, "Emissions of CO<sub>2</sub> in europe and the Asia–Pacific region: panel data model," *Energy Reports*, 8 894–901 (2022). doi:10.1016/j.egyr.2022.10.164.
- 9) G.A. Strategy, "Circular economy reinforcement to diminish ghg emissions: a grey dematel approach," *Evergreen*, 10 (01) 389–403 (2023). <https://doi.org/10.5109/6781099>
- 10) A. Wardoyo, and A. Budianto, "A DC low electrostatic filtering system for PM<sub>2.5</sub> motorcycle emission," *IEEE Xplore*, 1 51–54 (2017).
- 11) W.E. Cahyono, Parikesit, B. Joy, W. Setyawati, and R. Mahdi, "Projection of CO<sub>2</sub> emissions in indonesia," *Mater Today Proc*, 63 S438–S444 (2022). doi:10.1016/j.matpr.2022.04.091.
- 12) C.W.W. Ng, R. Tasnim, and J.L. Coo, "Effects of atmospheric CO<sub>2</sub> concentration on soil-water retention and induced suction in vegetated soil," *Eng Geol*, 242 (May) 108–120 (2018). doi:10.1016/j.enggeo.2018.06.001.
- 13) A.A. Widhowati, A.Y.P. Wardoyo, H.A. Dharmawan, M. Nurhuda, and A. Budianto, "Development of a portable volatile organic compounds concentration measurement system using a CCS811 air quality sensor," *IEEE Xplore*, 1–5 (2021). doi:10.1109/ISESD 53023.2021.9501642.
- 14) S. Subhashini, and A.V. Juliet, "Piezoresistive mems cantilever based CO<sub>2</sub> gas sensor," *Int J Comput Appl*, 49 (July) 5–10 (2012). doi:10.5120/7725-1128.
- 15) J. Kaur, V.I. Adamchuk, J.K. Whalen, and A.A. Ismail, "Development of an NDIR CO<sub>2</sub> sensor-based system for assessing soil toxicity using substrate-induced respiration," *Sensors (Switzerland)*, 15 (3) 4734–4748 (2015). doi:10.3390/s150304734.
- 16) A. Rianjanu, S.A. Hasanah, D.B. Nugroho, A. Kusumaatmaja, R. Roto, and K. Triyana, "Polyvinyl acetate film-based quartz crystal microbalance for the detection of benzene, toluene, and xylene vapors in air," *Chemosensors*, 7 (20) 1–9 (2019).
- 17) A. Mylonas, O.B. Kazanci, R.K. Andersen, and B.W. Olesen, "Capabilities and limitations of wireless CO<sub>2</sub>, temperature and relative humidity sensors," *Build Environ*, 154 (December 2018) 362–374 (2019). doi:10.1016/j.buildenv.2019.03.012.
- 18) A. Biadasz, M. Kotkowiak, D. Łukawski, J. Jadwiżak, K. Rytel, and K. Kędzierski, "A versatile gas transmission device with precise humidity control for QCM humidity sensor characterizations," *Measurement*, 200 (March) 111674 (2022). doi:10.1016/j.measurement.2022.111674.
- 19) A. Alassi, M. Benamar, and D. Brett, "Quartz crystal microbalance electronic interfacing systems: a review," *Sensors (Switzerland)*, 17 (12) 1–41 (2017). doi:10.3390/s17122799.
- 20) R. Aflaha, H. Afifyanti, Z.N. Azizah, H. Khoirudin, A. Rianjanu, A. Kusumaatmaja, R. Roto, and K. Triyana, "Improving ammonia sensing performance of quartz crystal microbalance (QCM) coated with nanofibers and polyaniline (PANI) overlay," *Biosens Bioelectron X*, 13 (October 2022) 100300 (2023). doi:10.1016/j.biosx.2022.100300.
- 21) D. Mardare, N. Cornei, C. Mita, D. Florea, A. Stancu, V. Tiron, A. Manole, and C. Adomnici, "Low temperature TiO<sub>2</sub> based gas sensors for CO<sub>2</sub>," *Ceram Int*, 42 (6) 7353–7359 (2016). doi:10.1016/j.ceramint.2016.01.137.
- 22) M.A. Raza, A. Habib, Z. Kanwal, S.S. Hussain, M.J. Iqbal, M. Saleem, S. Riaz, and S. Naseem, "Optical CO<sub>2</sub> gas sensing based on TiO<sub>2</sub> thin films of diverse thickness decorated with silver nanoparticles," *Advances in Materials Science and Engineering*, 2018 1–12 (2018). doi:10.1155/2018/2780203.
- 23) N.K. Yadav, N.S. Rajput, S. Kulshreshtha, and M.K. Gupta, "Investigation of the mechanical and wear properties of epoxy resin composite (ercs) made with nano particle TiO<sub>2</sub> and cotton fiber reinforcement," *Evergreen*, 10 (01) 63–77 (2023). <https://doi.org/10.5109/6781041>
- 24) J.Y. Lim, and S.S. Lee, "Quartz crystal microbalance cardiac troponin I immunosensors employing signal amplification with TiO<sub>2</sub> nanoparticle photocatalyst," *Talanta*, 228 (February) 122233 (2021). doi:10.1016/j.talanta.2021.122233.
- 25) A. Budianto, A.Y.P. Wardoyo, Masruroh, H.A.

Dharmawan, and M. Nurhuda, "Performance test of an aerosol concentration measurement system based on quartz crystal microbalance," *Journal of Physics: Conf. Series*, 1811 (1) 012033 (2021). doi:10.1088/1742-6596/1811/1/012033.

26) A. Budianto, A.Y.P. Wardoyo, H.A. Dharmawan, K.A. Hadi, and L. Mardiana, "Graphene oxide-coated quartz crystal microbalance for bioparticle detection (a case study for bacillus sp.)," *Evergreen*, 10 (01) 155–161 (2023). <https://doi.org/10.5109/6781066>

27) A. Budianto, R. Wirawan, R.R. Illahi, D.W. Kurniawidi, S. Rahayu, A.A.N.N. Kusuma, and A.T. Alaydrus, "A gravimetry-based fine particle concentration measurement system for humid environment using graphene oxide layer," *Evergreen*, 10 (3) 1414–1421 (2023). <https://doi.org/10.5109/7151690>

28) A. Budianto, A.Y.P. Wardoyo, Masruroh, and H.A. Dharmawan, "An airborne fungal spore mass measurement system based on graphene oxide coated QCM," *Pol J Environ Stud*, 31 (4) 3523–3529 (2022). doi:10.15244/pjoes/147057.

29) T.V.K. Karthik, L. Martinez, and V. Agarwal, "Porous silicon ZnO/SnO<sub>2</sub> structures for CO<sub>2</sub> detection," *J Alloys Compd*, 731 853–863 (2018). doi:10.1016/j.jallcom.2017.10.070.

30) D.B. Nugroho, A. Rianjanu, K. Triyana, A. Kusumaatmaja, and R. Roto, "Quartz crystal microbalance-coated cellulose acetate nanofibers overlaid with chitosan for detection of acetic anhydride vapor," *Results Phys*, 15 (September) 102680 (2019). doi:10.1016/j.rinp.2019.102680.

31) L. Mardiana, A.Y.P. Wardoyo, Masruroh, and H.A. Dharmawan, "A study of an n-TiO<sub>2</sub> coated QCM sensor's response and reversibility under CO<sub>2</sub> exposure," *Pol J Environ Stud*, 32 (2) 1735–1742 (2023).

32) J. Wang, and X. Guo, "Adsorption kinetic models: physical meanings, applications, and solving methods," *J Hazard Mater*, 390 122156 (2020).

33) C.E. Nanayakkara, W.A. Larish, and V.H. Grassian, "Titanium dioxide nanoparticle surface reactivity with atmospheric gases, CO<sub>2</sub>, SO<sub>2</sub> and NO<sub>2</sub>: Roles of surface hydroxyl groups and adsorbed water in the formation and stability of adsorbed products," *J Phys Chem*, 118 (40) 23011–23021 (2014). doi:<https://doi.org/10.1021/jp504402z>.